Diffusion of Seawater in Unsaturated Polyester Resin and Its Glass Fiber Reinforced Composites in the Presence of Titanium Dioxide as UV Absorber

M. V. Deepa Urs,[1] C. Ranganathaiah,[1] R. Ramani,[2] Babu Lal,[2] Sarfaraz Alam[2]

[1]*Department of Studies in Physics, University of Mysore, Manasagangotri, Mysore 570 006, India*
[2]*Polymer Science Division, DMSRDE, Kanpur 208 013, India*

Received 29 October 2005; accepted 3 November 2006
DOI 10.1002/app.24490
Published online in Wiley InterScience (www.interscience.wiley.com).

ABSTRACT: Diffusion of seawater in unsaturated polyester resin (UPR) and its glass fiber reinforced composite in the presence of titanium dioxide has been studied by sorption method. Incorporation of glass and TiO_2 to UPR alters the seawater diffusion process from Fickian to non-Fickian type. The dual mode sorption model is used to separate Fickian-controlled and relaxation-controlled diffusion in case of UPR-T, UPR-G, and UPR-GT. The presence of TiO_2 seems to stabilize UPR and its glass reinforced samples but an increase in the rate of seawater diffusion is observed for these systems. The free volume determined from positron lifetime measurements support the diffusion data in these systems. Results further indicate that the contribution to diffusion in the later stages of sorption is due to the increased contribution from the interfaces. The plasticizing effect of TiO_2 is clearly seen even in the glass reinforced composite. DMA results show an increase in flexibility because of TiO_2 presence both in the neat as well as glass reinforced resin which is well supported by decrease in T_g value from DSC data. © 2006 Wiley Periodicals, Inc. J Appl Polym Sci 102: 2784–2794, 2006

Key words: unsaturated polyester; glass fiber; seawater diffusion; positron lifetime; free volume; titanium dioxide

INTRODUCTION

Polymers have been widely used in aerospace as well as in transport industries for a veriety of applications including structural forming materials. To meet the increasing demand on various working environments and at the same time to reduce the cost, polymers have been tried with the addition of suitable fillers and/or fibers to enhance their overall performance in terms of mechanical, electrical, and photonic properties, and structural stability.[1] The addition of reactive inorganic fillers can considerably modify their solvent resistivity because of strong bonding between fillers and diffusive liquids.[2]

The glass–fiber reinforced polymer (GRP) composite has been proposed and tried for critical marine components such as masts, submarine control surfaces, transmission shafts and propellers. This follows the application of GRP composites in primary structures of ships including hull, decks and structural bulkheads, and also to superstructure, nonstructural bulkheads, submarine casings, sonar domes, and radomes etc. Polyester laminates are considered better for ship primary structural applications because of their higher mechanical properties and cheaper cost over phenolic laminates.[3] The polymer matrix in all GRP composites for seawater applications is either isophthalic polyester or vinyl ester resin.[4] When used in marine applications, it is essential that these composites retain their mechanical properties to the maximum possible level and do not degrade over prolonged usage. The degradation of these composites arises mainly due to seawater diffusion, UV irradiation from sun light and microorganisms in seawater. However, when the ship is stationary for a long period in the port, the degradation due to microorganism would be minimum. Introduction of UV absorbing material to the resin matrix is expected to reduce its degradation because of UV irradiation. A concern in using the materials with UV absorbers is the influence of these UV absorbers on the seawater diffusion behavior of the resins and composites. Studies on the nature of seawater transport at the molecular level in polyester resins and laminates with UV absorbers are scanty and such a study would give an idea about their actual usage in marine applications and hence the present study.

In the present study, we have incorporated a transition *d*-block metal oxide, namely titanium dioxide (TiO_2), a UV absorbing material to unsaturated polyester resin (UPR). In case of glasses, TiO_2 is known to be a network-former and/or network-modifier.[5] It is of interest to find how the TiO_2 modifies the structure of

Correspondence to: C. Ranganathaiah (cr@physics.uni-mysore.ac.in).

UPR and its glass reinforced composites at the molecular level, and how this modification in turn would affect the seawater diffusion in them. Diffusion in polymer resins heavily depends on free volume.[6,7] So, the free volume fraction becomes a measure of the ability of the medium to sorb seawater. Free volume cavities provide the express pathway for diffusion. Thus the efficient means of understanding the diffusion process in polymers is by studying their free volume fraction and how it controls diffusion of different species. The free volumes or the open spaces are the regions present in the amorphous domains of the polymer system. The existence of free volume holes in polymers was proposed to explain the molecular motion and physical behavior of glassy and liquid states.[6] One of the most versatile experimental methods by which one can measure this nanometer sized free volume cavities and their content in a polymer at present is positron lifetime spectroscopy (PLS). The topology of the polymer, which influences the kinetics of seawater transport, can be quantified via the PLS in terms of size and volume fraction of the free volume. Topology here means the spatial or geometrical characteristics of connect crosslink structure. Different topologies can lead to more open structure that would be more amenable to the transport of small molecules such as seawater.

In the present study, we have used this novel technique to unravel, how the nano voids influence the seawater diffusion in the composites.[8] It should be noted here that the use of this novel technique to understand the properties of composite materials is very scanty.[9,10] Furthermore, the long-range cooperative molecular motions dominate mechanical properties both in the viscous and solid state and can be characterized by dynamic mechanical analysis (DMA).[11] Since the molecular motions result to change in free volume, which in turn is related to diffusion as well as changes in dynamic and other mechanical properties.[12,13] Therefore, we have carried out DMA, positron measurements, and sorption of seawater to look for a correlation, if any among these parameters. Thus, in the present study we have been motivated to understand seawater diffusion process in UPR and its glass fiber reinforced composite upon TiO_2 addition and probe the molecular origins of changes in mechanical properties. Seawater sorption is carried out by conventional gravimetric method. In the present investigation, seawater sorption was examined in three composite laminates as described under materials section.

MATERIALS

Sample preparation

The isophthalic UPR and the curing agents used in the present study were obtained from M/s Bakelite Hylam, Hyderabad, India. The UPR was reinforced with E-glass plain woven fabric supplied by M/s. Unnati, India. The fabric had an average filament diameter of about 12 μm and an aerial weight of 0.360 kg/m^2. These glass fibers, as supplied, were coated with an emulsion based sizing agent to promote good chemical adhesion to the resin matrix. The UPR is a highly crosslinked thermosetting polymer and can be easily cured at room temperature. Pure and TiO_2 filled UPR sheets were prepared as follows: titanium dioxide (TiO_2), obtained from Kerala Mines and Minerals, India was used as the filler. Exactly, 5 wt % of TiO_2 was added to UPR and mechanically mixed in a glass beaker for approximately 10 min. The mixture was placed in a vacuum chamber at 28 Torr for 5 min to remove trapped air bubbles generated during the mechanical mixing process. The resin was accelerated with 1.25 wt % cobalt octate and catalyzed with 1.25 wt % methyl ethyl ketone peroxide (MEKP) solution and mixed thoroughly. The mixture was then deaerated again for a short time to remove the air bubbles, if any. The second deaeration process needs to be very quick as polymerization commences almost instantaneously once the catalyst is added. The final mixture was poured into a rectangular mold coated with a mold release agent. To prevent the particle settlement at the bottom, the mold was rotated at 2 rpm for at least 4 h until the mixture was rigid enough so that the particles could no longer migrate. The resin mixture was allowed to cure at room temperature with suitable pressure for 48 h. After this, the specimen was post cured in an air-circulating oven for 3 h at 100 °C.

The pure and TiO_2 filled UPR were used to prepare glass fiber reinforced laminates using the wet hand lay-up process. The woven glass fabric was chopped into 7 × 10 in. pieces. Resin was applied to the bottom of the mold by a roller followed by the first layer of the chopped woven fabric. To obtain a homogeneous laminate free from bubbles, sufficient resin was always placed in the mold and rolling would displace the entrapped air from the laminate. Twelve such layers of resin and chopped woven fabric were successively applied using the same technique. Finally the mold was closed and sufficient pressure was applied and kept at room temperature for 48 h for curing. Postcuring was performed in a similar manner as explained earlier for the nonglass reinforced sheets. The cured sample was taken out from the oven and demolded after the oven attains room temperature. The so fabricated sheets and laminates of ~4 mm thickness were kept at room temperature for few weeks before being cut to various shapes for mechanical and other characterizations. The resin content of the glass reinforced laminates was determined by resin burning off to be 39% ± 1%

by weight. The sample so prepared are labeled as (1) neat UPR, (2) UPR filled with 5% TiO_2 (UPR-T), (3) 60% glass fiber reinforced UPR laminate (UPR-G), and (4) 60% glass fiber reinforced UPR filled with 5% TiO_2 laminate (UPR-GT).

EXPERIMENTAL TECHNIQUES

Brief description of PLS

The basis of PLS involves the injection of positrons from a radioactive source into the material under study. Positrons thermalize very rapidly through interactions with the surrounding molecules and these thermalized positrons annihilate with electrons of the medium. A positron can annihilate from different states in a medium. In molecular media like polymers, it can form a bound state called Positronium (Ps). The Ps exists in two states, depending on the relative spin of the positron and the electron. The *para*-Positronium (*p*-Ps) with spins antiparallel has a lifetime of 125 ps and it annihilates with the emission of two γ photons. The *ortho*-Positronium (*o*-Ps), with parallel spins has a longer lifetime and annihilates in free space into three γ photons with a lifetime of 140 ns. In polymers, *o*-Ps annihilates predominantly via a fast channel, called pick-off annihilation (positron of *o*-Ps annihilates with an outside electron from the medium having opposite spin) by two γ photon emission and its lifetime gets reduced to a few nanoseconds. The *o*-Ps pick-off lifetime therefore is a measurable parameter, which depends on the overlap of the Ps wave function with the wave function of the electrons of the medium. The *o*-Ps gets localized in free volume cavities like positrons localize in defects before annihilation. So, its lifetime is a measure of the free volume cavity size and in terms of probability of the *o*-Ps intensity. Is a measure of relative number of these cavities. Larger the cavity size, smaller is the overlap of the wave functions, and longer is the *o*-Ps lifetime.[14] The formation of *o*-Ps and its yield in polymers is determined by the positron lifetime measurement, attributing the long-lived component to the *o*-Ps decay, which provides information on the free volume holes in the polymer matrix.[7]

Positron lifetime measurements

Positron lifetime measurements were carried out using a fast–fast coincidence system with conically shaped BaF_2 scintillators coupled to photomultiplier tubes type XP2020/Q with quartz window as detectors. ^{22}Na positron source of 17 μCi was used in the present experiment. Two identical samples of 1.5 mm × 1.5 mm × 2 mm were cut from the demolded laminate and placed on either side of the positron source (standard sandwich geometry was employed). This sandwich was placed between the two detectors of the positron lifetime spectrometer for lifetime measurements. For each sample, two to three positron lifetime spectra with more than one million counts under each spectrum were recorded. Source contribution and resolution functions were estimated from the lifetime of well-annealed aluminum using the program RESOLUTION.[15] A time resolution of 220 ps was obtained using three Gaussian resolution functions, which gave better convergence of the spectrum. More details on the instrumentation and spectrum analysis can be found elsewhere.[15] The lifetime spectrum so acquired was analyzed into two and three components using PATFIT-88 computer program.[16] Though three-component analysis gave convergence to moderately acceptable level, the intensity of the third lifetime component was around 1% in all these samples. This is very small compared to surface annihilation contribution and hence neglected. Hence only two-component analysis results, which gave better χ^2 values and standard deviations than three-component analysis, are reported here. All measurements were performed at room temperature.

Seawater sorption measurements

For sorption measurements natural seawater (collected from Bay of Bengal) with salinity content of about 4.6% was used in the present study. Sorption of seawater was carried out at room temperature by soaking the samples in seawater for different intervals of time. After each sorption time, the samples were withdrawn from seawater, blotted with a blotting paper for removal of surplus seawater on the surface and weighed using a Mettler digital balance to an accuracy of 100 μg to monitor the mass change in them. An important point to be noted here is that both the faces of the composite specimens were exposed to seawater. In the actual service conditions, however, the seawater diffusion is only from one side. Moreover, these specimens do not have a gel coat on them like the composites used in actual seawater applications. Therefore the present results could be taken as to represent an unusually severe condition.

DMA measurements

Dynamic mechanical measurements were carried out using a Dynamic mechanical analyzer of TA instruments (model no. 2980). Dimensions of a typical sample were 65 mm × 12 mm × 4 mm (length × width × thickness) and the measurements were carried out under tensile test mode at a frequency of 1 Hz from room temperature to 170°C with a heating rate of 5°C/min.

DSC measurements

The DSC scans were taken from a differential scanning calorimeter of TA instruments (model no. 2920) using ~ 5 mg of the sample with a heating rate of 5°C/min and a nitrogen purge gas at a flow rate of 40 mL/min.

RESULTS AND DISCUSSION

DSC results

The DSC scans are not shown but results derived from these namely the glass transition temperature (T_g) are tabulated in Table I. The middle of the transition was taken as T_g. From the table, we see that the T_g of neat UPR is 74°C and is in close agreement with literature data.[17] This T_g gets shifted to 71°C in UPR-T, revealing the plasticizing action of TiO_2. However, glass fiber reinforced UPR shows that T_g increases to 95°C, suggesting the effectiveness of the glass fiber as a reinforcing agent which means that the UPR and glass fiber interfacial interaction is higher in this case. On the other hand, when TiO_2 is added to glass fiber reinforced UPR, this brings down the T_g value to 86°C, which further reiterates the plasticizing effect of TiO_2.

DMA results

The DMA results can be explained in terms of three parameters, storage modulus (SM, E'), loss modulus (LM, E'') and the damping peak (tan δ). The SM E' is the elastic response of the material whereas the LM (E'') is the viscous response of the material. The damping peak (tan δ) is simply the ratio of LM (E'') to SM (E') and is a measure of flexibility of the material. The tan δ peak occurs in the region of glass transition, where the material changes from the rigid phase to more flexible rubbery state and is associated with the movement of small groups and chains of molecules within the polymer structure, all of which are frozen in below T_g.

To understand the nature of the samples under study at room temperature, their storage and LM values are tabulated in Table I. The E' value of the neat UPR gets lowered after TiO_2 addition (sample UPR-T). This lowering of modulus value may be due to the dilution of the polymer. After glass reinforcement (UPR-G), the E′ value becomes higher compared to neat UPR.

The glass transition temperature T_g can be also be determined with significant levels of sensitivity through DMA by monitoring the changes in the LM maximum or tan δ as a function of temperature. It is noted that the T_g indicated by the use of the maximum value of E'' peak is lower than tan δ peak. This is because E'' maximum occurs in the middle of the transition whereas tan δ peak occurs at the end of the transition region. However, there is an argument with regard to the consideration of T_g from DMA results whether to consider E' peak values or tan δ peak values, particularly in polymer composites.[18,19] The authors in reference R1 argue that LM peak value indicates more precisely the temperature at which the stiffness suffers significant deterioration and need to be considered as the true T_g value. In our case, LM peak temperature values are in close in agreement with the DSC results and hence they are considered. However, the tan δ peak temperature is found to be lower for UPR-G as compared to neat UPR.

The magnitude of tan δ peak is indicative of the nature of the polymer system. Improvement in interfacial bonding in composites occurs if the lowering of tan δ value is observed.[12] The higher the damping at the interfaces, poorer is the interfacial adhesion. From Table I, we see that the tan δ peak value gets reduced in UPR-T and UPR-G as compared to UPR. The reason for this reduction is the incorporation of fillers and fibers which reduce the tan δ peak height by restricting the movement of polymer molecules. In UPR-G, lowering of tan δ value is mainly due to the reinforcing action of fiber and shear stress concentrations at the fiber ends. However, there is a slight increase in its value in case of UPR-GT as compared to UPR-G. The formation of Ti—O—Si type bonds in UPR-GT system seems to deteriorate the interfacial adhesion between the glass fiber and the UPR matrix as well as the reinforcing action of glass fiber. This aspect is further strengthened by the decrease in T_g value for UPR-GT as compared to UPR-G (Table I).

A correlation is observed from the values of SM and LM and the T_g values of these samples. Upon TiO_2 addition to UPR (sample UPR-T), the SM decreases by 1.69 times while LM decreases only by

TABLE I
Results of DMA and DSC Measurements

Sample	E' (MPa)	E'' (MPa)	LM (peak temp in °C)	tan δ (peak temp in °C)	tan δ peak ht (cm)	DSC (T_g °C)
UPR	2143	100	73	125	0.4789	74
UPR-T	1661	96.8	69	118	0.3254	71
UPR-G	10321	289	96	110	0.1763	95
UPR-GT	27642	2021	85	100	0.1891	86

1.03 times as compared to neat UPR. This suggests that there is an overall improvement in the flexibility of the system, which shall result in a decrease of the T_g. From Table I, it becomes clear that UPR-T has a lower T_g as compared to neat UPR. Upon glass reinforcement (sample UPR-G), the SM increases by 4.82 times while LM increases by 2.9 times as compared to their respective values for neat UPR. This indicates an overall improvement in the rigidity of the matrix with the incorporation of glass fibers into the UPR matrix. Thus on account of the reinforcing action of glass fibers in UPR, the stiffness of the matrix has increased. This effect is very well reflected by the increase in T_g value. The results of SM and LM are quite interesting when both glass fibers and TiO_2 are present in the composite. In comparison with UPR-G, there is an increase in both the modulus values (SM value by 2.7 times and LM value by 3.5 times) in UPR-GT. Since the loss factors are more sensitive to molecular motions, large increase in LM as compared to SM points to decreased constraints mainly in the amorphous domains of the system. The TiO_2 has a tendency to form chemical bond of the type Ti—O—Si on contact with silanol group.[20] If such a bond is formed in the present sample, the existing microstructure of the matrix certainly gets altered resulting to the observed change in modulus values. Thus we can conclude that there is an overall increase in flexibility in UPR-GT as compared to UPR-G, which is well supported by decrease in T_g values and increase in tan δ peak values (Table I).

Since TiO_2 is a good UV absorber and the above-mentioned data predict the formation of Ti—O—Si bonds, we therefore suppose that the structure stabilization against UV absorption is satisfactorily evident.

Positron lifetime results

The attribution of two lifetime components to various states of positron annihilation in the four samples of present study is as follows: the first lifetime τ_1 (around 280 ps) with its intensity I_1 is attributed to the contribution of *p*-Ps self annihilation and free positron annihilation. The second lifetime τ_2 (varies from 810 ps to 1005 ps) with intensity I_2 is attributed to *o*-Ps pick-off lifetime. Thermoset polymers, because of their highly crosslinked structure, are expected to contain small size free volume cavities.[21,22] as compared to thermoplastics like polycarbonate,[23] polyethyleneterephthalate,[23] polytetrafluoroethylene,[24] etc. The curing of UPR involves free-radical chain growth crosslinking and hence is expected to be highly crosslinked owing to its covalently bonded structure.[25] The *o*-Ps lifetime τ_2 is a measure of the average size of the free volume holes and I_2 represent the relative number density of these holes, which are mainly in the amorphous domains of the UPR matrix.[7]

The *o*-Ps lifetime τ_2 is related to the free volume hole size by a simple relation given by Nakanishi et al.,[26] which was developed based on the theoretical models of Tao[27] and Eldrup et al.[28] In this model, Ps is assumed to be localized in a spherical potential well having an infinite potential barrier of radius R_0. Also *o*-Ps is assumed to annihilate in a homogeneous electron layer of thickness ΔR (where $\Delta R = R - R_0$, R being the radius of the free volume) inside the well and the relation is

$$\tau_2^{-1} = 2[1 - (R/R_0) + (1/2\pi)\sin(2\pi R/R_0)]\text{ns}^{-1} \quad (1)$$

The parameter ΔR has been determined by fitting the experimental values of *o*-Ps lifetime obtained for molecular materials of known hole size like zeolites, and its value thus determined is 0.166 nm. This relation is used to calculate the average free volume radii of the four samples under study. Assuming these free volume cavities to be spherical, their average free volume size is evaluated as

$$V_f = (4/3)\pi R^3 \quad (2)$$

The summary of positron lifetime measurements and free volume data obtained from these measurements is provided in Table II. In polymer composites, which contain at least two different materials, the annihilation characteristics will be different. For samples having TiO_2 as filler, to account for the fraction of positrons, which annihilate in TiO_2, we have tried three positron lifetime component analysis with $\tau_2 = 329$ ps corresponding to positron lifetime in TiO_2 (from a separate positron lifetime measurement on pure TiO_2, we obtained $\tau_2 = 329$ ps with $I_2 = 59.4\%$) but the analysis yielded no convergence. Hence, we are of the opinion that 5% of TiO_2, added into the present systems contributes very little to positron lifetimes. This is because, once the TiO_2 is added to the UPR, this becomes a dispersed phase in the resin matrix. In such cases, what positron mostly encounters is the UPR matrix and not the dispersed TiO_2 particles.

It is evident from Table II, the free volume cavity size increases upon TiO_2 addition to UPR. However, the number density remains almost constant. This increased free volume is consistent with the increased flexibility of UPR-T given by DMA results.

TABLE II
Summary of Positron Lifetime Measurements

Sample	τ_2 (ps)	I_2 (%)	R (Å)	V_f (Å)^3
UPR	925 ± 10	5.82 ± 0.24	1.53 ± 0.002	15.03 ± 0.28
UPR-T	1005 ± 11	5.69 ± 0.18	1.67 ± 0.002	19.47 ± 0.37
UPR-G	946 ± 09	12.1 ± 0.24	1.57 ± 0.002	16.15 ± 0.26
URP-GT	810 ± 08	14.4 ± 0.34	1.31 ± 0.001	9.38 ± 0.16

The increased free volume size suggests that TiO_2 particles seem to act as spacers between UPR chains which results to increased free volume. Fillers are known to induce disruption in polymer chain packing.[29] Since the number of free volume sites remains almost constant upon TiO_2 addition to UPR, seems to suggest the formation of some interconnected free volume sites. Such a formation of interconnected microvoids has been proposed earlier in UPR/polyvinyl acetate system with $CaCO_3$ used as filler.[30]

In case of glass fiber reinforced composite, fraction of positrons can also form *o*-Ps and annihilate at the interface of the resin–glass fiber and thus can contribute to τ_2 and I_2. To account for the fraction of positrons which annihilate in the glass fibers, positron lifetime measurements were also performed on the glass fibers alone, which yielded $\tau_2 = 765$ ps and $I_2 = 24.7\%$. The E-glass fiber contains 55% SiO_2 as the main component with the reminder being oxides of other metals such as Al, Mg, and Ca, etc.[31] Generally, a composite is considered to have a matrix material (resin) surrounding it is the reinforced fiber, in which the two phases put together would produce characteristics not attainable by either constituent acting alone. When resin matrix is impregnated with these fibers, as like in TiO_2 powder, a layer of resin covers these fibers and hence the ultimate fate of positrons is that they annihilate in the resin matrix rather than with electrons from the glass fiber. Further, had there been a contribution from the glass fibers, the presence of the oxides would have reduced *o*-Ps lifetime since oxygen is a good quencher of *o*-Ps. On the contrary, the τ_2 value remains almost the same, suggesting that pure fiber contribution to final results would be negligible. However, the I_2 value shoots up to 12.1%, indicating that free volume cavities/interfaces upon glass reinforcement mainly from the interfaces have increased. In case of UPR-GT, since TiO_2 is a network former and/or modifier[5] as discussed earlier, it can form chemical bond of the type Ti—O—Si with the Silica of glass, thereby the oxide moieties of the glass fibers have a chance to get exposed even after resin treatment. Thus, owing to the quenching action (decrease of lifetime) of oxygen, the *o*-Ps lifetime decreases to 810 ps. The formation of such bonds might have resulted in increased *o*-Ps trapping centers, may be due to increased interfaces. As a result the I_2 value increases further. Thus, we can say in this complex matrix, positrons seem to preferably localize and annihilate in the free volume cavities of the resin and at the interfaces.

Seawater diffusion results

The sorption data is plotted and shown in Figures 1–4 for the four samples of study. From these moisture-uptake profiles, the diffusion coefficients can be easily calculated making use of the Fickian diffusion equation[32]

$$Q_t = \left(\frac{M_t}{M_\infty}\right) = 1 - \frac{8}{\pi^2}\sum_{n=0}^{\infty}\frac{1}{(2n+1)^2}\exp\left\{\frac{-(2n+1)^2\pi^2 Dt}{L^2}\right\} \quad (3)$$

where M_t is the moisture uptake at time t; M_∞, the equilibrium moisture uptake; L, the sample thickness; and D is the diffusion coefficient. This solution of Fick's second law holds true for the conditions of an infinite plane sheet maintained at a constant concentration. The ratio (M_t/M_∞) in eq. (3) is the quantity experimentally measured which can be expressed as

$$Q_t = (W_t - W_d)/(W_\infty - W_d) \quad (4)$$

where W_d is the weight of the dry sample; W_t, the weight of the sample that has been soaked in seawater for a time t; and W_∞ is the weight of the sample in the final stages of sorption. The ratio Q_t is evaluated according to the above equation with the measured values of W_t, W_d, and W_∞. A widely used approximation is the rule that at short time (up to $M_t/M_\infty = 0.5$), the amount of substance diffused is proportional to square root of the time of sorption, which is also known as the square-root-of-time-law or Stefan's approximation[32,33] and is given by

$$Q_t = 4[Dt/\pi L^2]^{1/2} \quad (5)$$

This approximation is derived under the assumption that the diffusion coefficient (D) is a constant. The diffusion coefficients can also be calculated from the late-time approximation of eq. (3) taking $n = 0$ which results in

$$Q_t = 1 - [(8/\pi^2)\exp[-D\pi^2 t/L^2] \quad (6)$$

A plot of Q_t versus square root of sorption time ($t^{1/2}$) is generally called the sorption curve, and D is calculated from the initial linear portion of this curve.

Figure 1 presents the sorption curve for UPR. The curve is linear during the early stages of sorption and reaches equilibrium at longer times, i.e., the ratio Q_t varies linearly with $t^{1/2}$ up to a value of $Q_t = 0.8$ and levels off at the final stages of sorption, which is characteristic of Fickian diffusion.[33,34]

Fickian diffusion is characterized by the rate of diffusion being much less than that of the polymer segmental relaxation, due to mechanical, structural and other such modes of penetrant–polymer system interaction. Non-Fickian type diffusion is that for

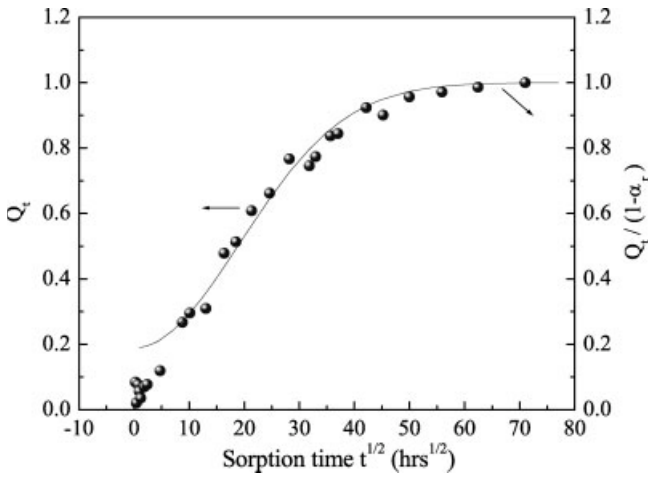

Figure 1 Variation of Q_t and $Q_t/(1-\alpha_r)$ as a function of square root of sorption time $t^{1/2}$ for UPR.

which the diffusion occurs faster than the segmental relaxation process and is hence termed relaxation-controlled diffusion.

Figures 2–4 demonstrate the respective sorption curves for UPR-T, UPR-G, and UPR-GT. At short times, the mass uptake Q_t increases linearly with $t^{1/2}$ indicating the Fickian behavior, but at longer times, the maximum uptake exhibits a protracted non-Fickian asymptotic approach towards equilibrium. So, there is a second stage of uptake showing an upward curvature, which is not a linear function of $t^{1/2}$.

Such anomalous kinetics of diffusion (two stage) coupling Fickian diffusion and polymer structural relaxation are often described using Berens and Hopfenberg model,[35] otherwise called dual mode sorption model. According to this model, the rapid Fickian diffusion process dominates the sorption at the initial stages of a penetrant-free polymer sample, while incremental sorption shows larger relative contributions from slow relaxation processes. The relaxation processes appear to be related to slow redistribution of available free volume through relatively large scale segmental motions in the relaxing polymer. Analysis of experimental sorption data through this model, yields kinetic and equilibrium parameters describing the individual contributions from the diffusion and relaxation process.[35] This model has been shown to provide a meaningful analysis of several non-Fickian 'anomalies', including a very slow approach to apparent equilibrium.[35,36] From the description of Fickian and non-Fickian (anomalous) sorption processes and a careful examination of the weight uptake plots in Figures 1–4, seawater sorption in UPR is pure classical Fickian diffusion whereas, for UPR-T, UPR-G, and UPR-GT, the sorption curves indicate anomalous diffusion (with continuing uptake rather than a plateau at longer immersion times), because of supplementary mechanisms, may be from interfaces which become dominant. Hence, we have used the dual mode sorption model to analyze the two-stage sorption kinetics in UPR-T, UPR-G, and UPR-GT. The analytical representation of this model, which explicitly separates contributions related to Fickian diffusion from those related to first order relaxation, is given by

$$Q_t = (1-\alpha_r)\left[1 - \frac{8}{\pi^2}\sum_{n=0}^{\infty}\frac{1}{(2n+1)^2}\exp\left\{\frac{-(2n+1)^2\pi^2 Dt}{L^2}\right\}\right] + \left[1-\alpha_r\exp\left(\frac{-t}{\tau_r}\right)\right] \quad (7)$$

where $(1-\alpha_r)$ and α_r are the fractions of mass uptakes in the overall sorption contributed by Fickian diffusion and relaxation respectively, and τ_r is the first-order time constant associated with the long time drift in mass uptake. The long time drift in sorption kinetics is usually ascribed to mass uptake controlled by the viscoelastic relaxation of the polymer chains to accommodate penetrant.[36] This model represents diffusion and relaxation as parallel processes and the faster process controls the initial mass uptake. On the basis of the linearity of initial mass uptake with $t^{1/2}$ in Figures 3 and 4, Fickian diffusion seems to control the initial mass uptake in all the cases. Since rate of sorption in the initial stage is controlled by Fickian diffusion, this initial portion may be used to estimate the diffusion coefficient even when the total sorption does not follow the Fickian model.[37] Hence the Fickian diffusion coefficients for UPR-T, UPR-G, and UPR-GT, are estimated from the slope of the linear regions of their sorption curves in Figures 1–4 and the best fitted values of D are tabulated in Table III.

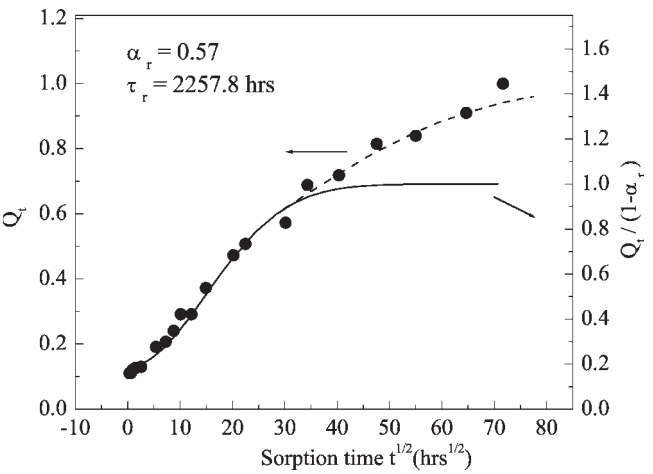

Figure 2 Variation of Q_t and $Q_t/(1-\alpha_r)$ as a function of square root of sorption time $t^{1/2}$ for UPR-T. (●) represent the experimental points; (—) is a fit to part I of eq. (7); and (– – –) is a fit to part II of eq. (7).

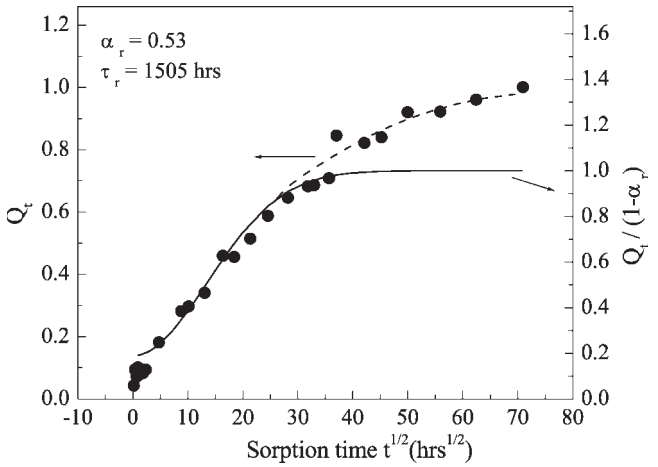

Figure 3 Variation of Q_t and $Q_t/(1-\alpha_r)$ as a function of square root of sorption time $t^{1/2}$ for UPR-G. (●) represent the experimental points; (—) is a fit to part I of eq. (7); and (– – –) is a fit to part II of eq. (7).

To separate the pure Fickian contribution in the sorption curves, the experimental data were fitted to the model for diffusion in a uniform plane sheet[30]

$$\frac{Q_t}{(1-\alpha_r)} = 1 - \frac{8}{\pi^2}\sum_{n=0}^{\infty}\frac{1}{(2n+1)^2}\exp\left\{\frac{-(2n+1)^2\pi^2 Dt}{L^2}\right\} \tag{8}$$

which is nothing but the first part of eq. (7).The solid curves in Figures 1–4 represent this fit and corresponds to pure Fickian contribution to seawater sorption in these samples.

In the spirit of the model embodied in eq. (7), relaxation controlled mass uptake is described as a single exponential,

$$\ln(1-Q_t) = \ln\ \alpha_r - (t/\tau_r) \tag{9}$$

To separate relaxation contribution to the seawater sorption kinetics, graphs of ln $(1-Q_t)$ versus sorption time t are drawn for the samples UPR, UPR-T, and UPR-GT. Then the time constant τ_r, characterizing the non-Fickian drifts in mass uptake towards equilibrium after the initial diffusion controlled regime, for each case is found from the inverse of slope of these graphs. Further, the intercepts of these plots yield the respective α_r values. The parameter values so obtained are recorded in Table III. The dashed curves in Figures 2–4 represent the fit to the experimental data with these calculated values of τ_r and α_r.

Now, it becomes evident from diffusion and relaxation separated curves, sorption remains Fickian upto 43, 47, and 41% for UPR-T, UPR-G, and UPR-GT respectively. The incorporation of glass and TiO_2 changes the mode of diffusion to non-Fickian type. Though there is not much change in percentage Fickian contribution, it can be observed that as small as 5% of TiO_2 addition appears to change the Fickian diffusion to a greater extent than 60% of glass fiber in UPR. The diffusion of seawater in UPR-G in the present case is 125 cm^2/s, which is very much less compared to 228 cm^2/s reported in literature.[3] Although the curing agents used in the present study and Ref. [3] were the same, the proportion is little different which seems to be crucial from the point of view of crosslinking. Further, in our case, post curing was done at 100°C, whereas in Ref. [3], the authors carried out post curing at 70°C. Higher the curing temperature, higher is the crosslink and this increased crosslink is the cause of reduced diffusion rate.

From the combined PLS, DMA, and sorption results, TiO_2 addition in UPR seems to have created some interconnecting free volume cavities because of which the size of cavities have increased. As such the rate of diffusion has increased from 79 to 152.8 cm^2/s in case of UPR-T. Once the preexisting free volume cavities get filled, the Fickian diffusion has changed to non-Fickian type, where the diffusion at interfaces becomes significant. This implies that TiO_2 sits at the interfacial region of chain segments thus enhancing the free volume size and probably interfaces. These effects are reflected in the increased free volume size (τ_2) in case of UPR-T. DSC results clearly indicate the plasticizing action of TiO_2 through reduction in its T_g (sample UPR-T vis-à-vis UPR), which also contributes to the increasing permeation rate. The process of relaxation involves tension between the swollen and un-swollen parts of the polymer because the latter resists further swelling. The presence of TiO_2 seems to hinder the segmental motion of the chains and

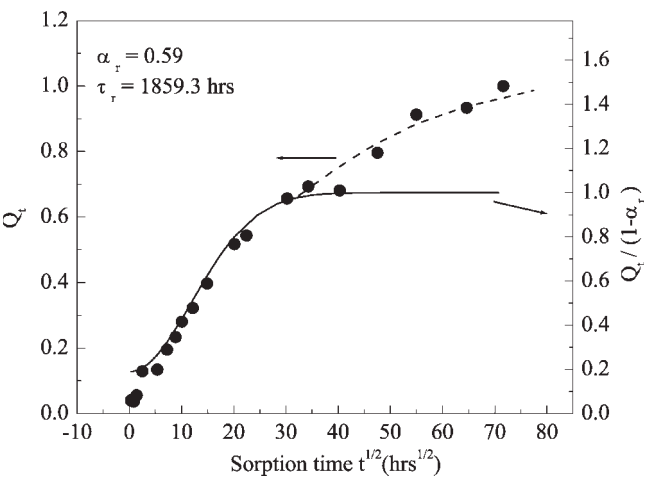

Figure 4 Variation of Q_t and $Q_t/(1-\alpha_r)$ as a function of square root of sorption time $t^{1/2}$ for UPR-GT. (●) represent the experimental points; (—) is a fit to part I of eq. (7); and (– – –) is a fit to part II of eq. (7).

TABLE III
Summary of Seawater Sorption Measurements

Sample	Sorption type	% of Fickian	% of max wt gain	$D \times 10^{10}$ (cm^2/s)	τ_R (h)	α_R	$1-\alpha_R$
UPR	Fickian	100	1.25	79.0	0.0	0.0	1.00
UPR-T	Non-Fickian	43	1.00	152.8	2257.8	0.57	0.43
UPR-G	Non-Fickian	47	2.20	125.0	1505.0	0.53	0.47
URP-GT	Non-Fickian	41	5.7	167.0	1859.3	0.59	0.41

restricts the chain segments to reach their equilibrium position. This is reflected from the measured larger structural relaxation time constant τ_r of 2257.8 h and decreased tan δ peak height in UPR-T as compared to neat UPR.

The incorporation of glass fiber as reinforcement reduces the segmental motion and hence the tan δ peak height falls almost 1/3 to its original value. However, in case of UPR-G, although there is not much change in the free volume cavity size, the rate of diffusion enhances compared to neat resin. This is probably due to creation of the additional free volume sites (I_2 increases), which are formed upon glass reinforcement in UPR. In case of UPR-GT the free volume cell size decreases but there is an increase in the number of free volume sites and hence the rate of seawater diffusion increases. This can be seen as the plasticizing action of TiO_2 as we noticed in the case of UPR-T. The possible formation of Ti—O—Si type bonds in UPR-GT system seems to increase the tension between the swollen outer part and the rigid core. Hence τ_r is higher in UPR-GT when compared to UPR-G. The relaxation contribution to diffusion ($\alpha_r = 0.59$) in UPR-GT is greater than in UPR-G ($\alpha_r = 0.53$). Similar effect is also reflected in the observed high value of E' in UPR-GT (Table I).

To illustrate the effect of fibers and interfaces on the seawater uptake in glass reinforced polyester, the uptake data were normalized on the basis that no fiber was present and this is presented in Figures 5 and 6 as attributed uptake for the matrix in glass fiber reinforced laminate. As can be seen from these, in both UPR-G and UPR-GT, the uptake occurs marginally faster for the glass reinforced laminates (UPR-G and UPR-GT) than for the neat resins (UPR and UPR-T). The fast uptake for the glass reinforced laminates than neat resins is reflected in a fast attributed uptake for the matrix in glass reinforced laminates. This higher attributed uptake for matrix in UPR-G and UPR-GT can be interpreted as the dominance of free volume over interface effects. From positron results it is clear that, upon glass reinforcement (sample UPR-G), the free volume number density (I_2) increases by 6.3% as compared to pure UPR. Similarly, in case of UPR-GT, I_2 increases by 8.7% compared to UPR-T. This high porosity, in case of glass reinforced samples is due to the interlaminar spacing, which is responsible for enhanced water uptake. Such a kind of dominance of free volume over interface effects in enhancing uptake has been reported for carbon/epoxies.[36] Absorption enhancement due to void content has been described by Thomason[38] for a range of glass–epoxy composites exposed to 100% humidity. Direct linear proportionality was reported between void level and both the rate of uptake and the peak uptake. Void content was reported to be more significant than interfaces in enhancing absorption.[36] This could also be the reason for high rate of seawater uptake of 2.2% in case of UPR-G compared to 1.25% in UPR and 5.7% in case of UPR-GT when compared to 1.0% in UPR-T.

Possible fiber related mechanisms include transport along the interfaces or continuing diffusion through the matrix with accumulation at the boundaries of the fibers. Ashbee and Wyatt.[39] proposed osmosis at the interface by alkali metal oxides leaching from E-glass in the presence of moisture to form concentrated salt solutions. They opined that concentration gradient would drive further diffusion of water towards the interface. Further it was illustrated, etching on the surface of fibers and differentiated three glass fiber types on the basis of correlations between alkali content and fiber debonding considered to result from osmotic pressure. Debonding from this process would further

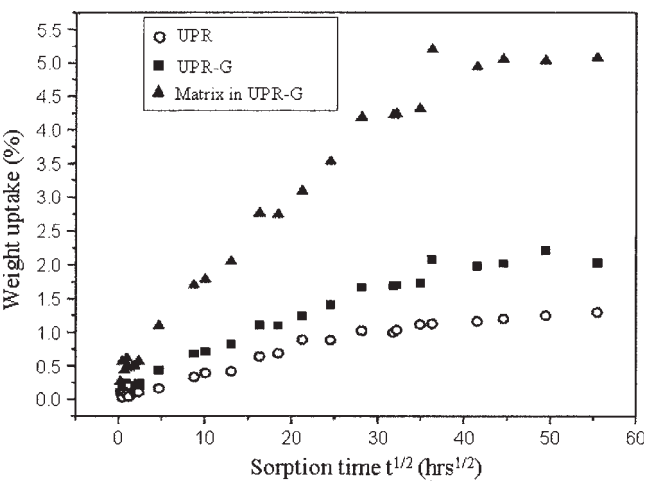

Figure 5 Weight uptake (%) of UPR and UPR-G with the attributed uptake for the matrix in UPR-G based on the resin proportion.

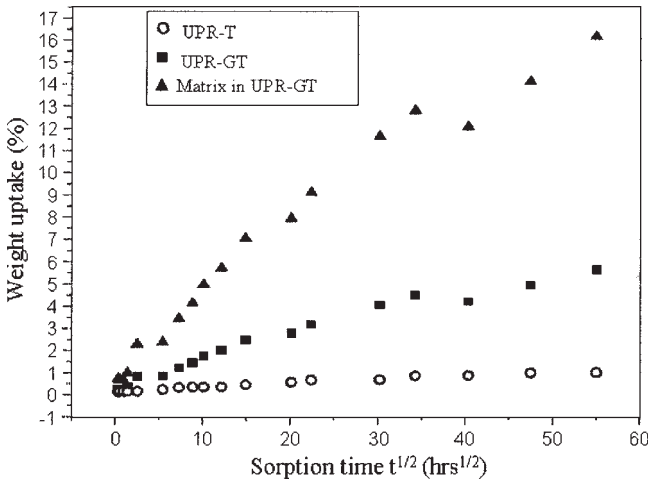

Figure 6 Weight uptake (%) of UPR-T and UPR-GT with the attributed uptake for the matrix in UPR-GT based on the resin proportion.

assist water transport along interfaces. Such osmotically enhanced uptake would be manifest later rather than earlier in the uptake history, consistent with the second stage uptake in both UPR-G and UPR-GT, which is dominated by relaxation controlled diffusion, in the present study.

Hence, it is very clear from sorption results, the initial mass uptake in glass reinforced samples, is through free volume in matrix and interlaminar spaces, which is indicated by Fickian behavior. On the other hand the second stage uptake is non-Fickian diffusion dominated by contribution from interfaces.

CONCLUSIONS

From the seawater diffusion study in UPR and its glass reinforced composites, we see that the sorption mechanism for pure UPR follows typical Fickian diffusion. The incorporation of glass and TiO_2 changes the mode of diffusion to non-Fickian type. The Fickian and relaxation contribution to diffusion have been analyzed using the dual mode sorption model. Though there is not much change in percentage Fickian contribution, TiO_2 addition appears to change the Fickian diffusion to a larger extent than glass fiber in UPR. The UV absorber TiO_2 acts as spacer and seems to have created some interconnecting free volume cavities increasing the rate of diffusion in UPR-T as compared to pure UPR. Glass reinforcement also results in increased diffusion rate through increase in free volume density due to interlaminar spacing. Once the preexisting free volume cavities get filled, the Fickian diffusion changes to non-Fickian type, where the diffusion at interfaces becomes significant. The sorption results correlate very well with the positron, DMA and DSC results.

Though TiO_2 leads to structure stabilization against UV irradiation through Ti—O—Si bond formation, it also increases the seawater diffusion in the UPR composites. Therefore this research is still open to find out the behavior of TiO_2 in other composites might lead to a better way of using TiO_2 as UV absorber in marine applications.

One of the authors (M.V.D.) is thankful to the University of Mysore, Manasagangotri, Mysore -570 006, India for providing financial support. The authors thank Mr. G.D. Pandey and his team, Central Analytical Facility, DMSRDE, Kanpur, India for their help in DMA and DSC measurements.

References

1. Selley, J. Encyclopedia of Polymer Science and Engineering; Wiley: New York, 1988.
2. Lungu, A.; Mejiritski, A.; Neckers, D. C. Polymer 1998, 39, 4757.
3. Gellert, E. P.; Turley, D. M. Compos A 1999, 30, 1259.
4. Smith, C. S. Design of Marine Structures in Composite Materials; Elsevier Applied Science: London, 1990.
5. Watanabe, N.; Ramos, A. Y.; Alves, M. C. M.; Tolentino, H.; Alves, O. L.; Barbosa, L. C. J Mater Res 2000, 15, 793.
6. Doolittle, A. K. J Appl Phys 1951, 22, 1471.
7. Jean, Y. C. Microchem J 1990, 42, 72.
8. Brydson, J. A. Plastic Materials; Iliffe Books: London, 1969.
9. Dale, J. M.; Hulett, L. D; Rosseel, T. M.; Fellers, J. F. J Appl Polym Sci 1987, 33, 3055.
10. Simon, G. P. Trends in Polym Sci 1997, 5, 394.
11. Davis, W. J.; Pethrick, R. A. Polymer 1998, 39, 255.
12. Pothan, L. A.; Oommen, Z.; Thomas, S. Compos Sci Technol 2003, 63, 283.
13. Blackwood, K. M.; Pethrick, R. A.; Simpson, F. I.; Day, R. E.; Watson, C. L. J Mater Sci 1995, 30, 4435.
14. Brandt, W.; Berko, S. Walker, W. W. Phys Rev B: Condens Matter 1960, 120, 1289.
15. Ravikumar, H. B.; Ranganathaiah, C.; Kumaraswamy, G. N.; Thomas, S. Polymer 2005, 46, 2372.
16. Kirkegaard, P.; Pederson, N. J.; Eldrup, M. PATFIT-88; Riso National Laboratory: Denmark, 1989.
17. Yinghong, X.; Xin, W.; Xujie, Y.; Lude, L. Mater Chem Phys 2002, 77, 609.
18. Akay, M. Compos Sci Technol 1993, 47, 419.
19. Karbhari, V. M.; Wang, Q. Compos B 2004, 35, 299.
20. Masuda, Y.; Saito, N.; Hoffmann, R.; De Guire, M. R.; Koumoto, K. Sci Technol Adv Mater 2003, 4, 461.
21. Ranganathaiah, C.; Sprinkle, D. R.; Pater, R. H. NASA Technical Memorandum 4707, 1996.
22. Alegaonkar, P. S.; Bhoraskar, V. N. Radiat Eff Defects Solids 2004, 159, 511.
23. Ramani, R.; Ranganathaiah, C. Polym Int 2001, 50, 237.
24. Ramani, R.; Ramachandra, P.; Ramgopal, G.; Ravichandran, T. S. G.; Ranganathaiah, C.; Gopal, S. Phys Status Solidi A 1996, 158, 1.
25. Evora, V. M. F.; Shukla, A. Mater Sci Eng A 2003, 361, 358.
26. Nakanishi, H.; Wang, S. J.; Jean, Y. C. In Positron Annihilation in Fluids; Sharma, S. C., Ed.; World Scientific: Singapore, 1988; p 292.
27. Tao, S. J. J Chem Phys 1972, 56, 5499.

28. Eldrup, M.; Lightbody, D.; Sherwood, J. N. Chem Phys 1975, 11, 129.
29. Merkel, T. C.; Freeman, B. D.; Spontak, R. J.; He, Z.; Pinnau, I.; Meakin, P.; Hill, A. J. Chem Mater 2003, 15, 109.
30. Zhang, Z.; Zhu, S. Polymer 2000, 41, 3861.
31. Ishida, H.; Koenig, J. L. Polym Eng Sci 1978, 18, 128.
32. Crank, J. The Mathematics of Diffusion, 2nd ed.; Clarendon Press, Oxford Scientific publications: Oxford, 1975; p 414.
33. Turner, D. T.; Abell, A. K. Polymer 1987, 28, 297.
34. Aithal, U. S.; Aminabhavi, T. M.; Cassidy, P. E. J Membr Sci 1990, 50, 225.
35. Berens, A. R.; Hopfenberg, H. B. Polymer 1978, 19, 489.
36. McDowell, C. C.; Freeman, B. D.; McNeely, G. W. Polymer 1999, 40, 3487.
37. Berens, A. R. Polymer 1977, 18, 697.
38. Thomason, J. L. Composites 1995, 26, 477.
39. Ashbee, K. H. G.; Wyatt, R. Proc R Soc London Ser A 1969, 312, 553.